Ann. Geophys., 24, 1493–1510, 2006
www.ann-geophys.net/24/1493/2006/
© European Geosciences Union 2006

Annales Geophysicae

Study of desert dust events over the southwestern Iberian Peninsula in year 2000: two case studies

V. E. Cachorro[1], R. Vergaz[1,*], A. M. de Frutos[1], J. M. Vilaplana[2], D. Henriques[3], N. Laulainen[4], and C. Toledano[1]

[1]Grupo de Optica-Atmosférica, GOA-UVA, Universidad de Valladolid, Spain
[2]ESAT-El Arenosillo-INTA, Huelva, Spain
[3]Instituto de Meteorologia de Portugal, Lisboa, Portugal
[4]PNNL, Pacific Northwest National Laboratory, Richland, WA, USA
[*]now at: Dpto. Tecnología Electrónica, Universidad Carlos III, Madrid, Spain

Received: 13 June 2005 – Revised: 16 February 2006 – Accepted: 28 February 2006 – Published: 3 July 2006

Abstract. Strong desert dust events occurring in 2000 over the southwestern Atlantic coast of the Iberian Peninsula are detected and evaluated by means of the TOMS Aerosol Index (A.I.) at three different sites, Funchal (Madeira Island, Portugal), Lisboa (Portugal) and El Arenosillo (Huelva, Spain). At the El Arenosillo station, measurements from an AERONET Cimel sunphotometer allow a more precise retrieval of the spectral AOD and the derived alpha Ångström coefficient. After using different threshold values of these parameters, we conclude that it is difficult to establish reliable and robust criteria for an automatic estimation of the number of dust episodes and the total number of dusty days per year. As a result, additional information, such as airmass trajectories, were used to improve the estimation, from which reasonable results were obtained (although some manual editting was still needed). A detailed characterization of two selected desert dust episodes, a strong event in winter and another of less intensity in summer, was carried out using AOD derived from Brewer spectrometer measurements. Size distribution parameters and radiative properties, such as arefractive index and the aerosol single scattering albedo derived from Cimel data, were analyzed in detail for one of these two case studies. Although specific to this dust episode, the retrieved range of values of these parameters clearly reflect the characteristics of desert aerosols. Back-trajectory analysis, synoptic weather maps and satellite images were also considered together, as supporting data to assess the aerosol desert characterization in this region of study.

Keywords. Atmospheric composition and structure (Aerosols and particles; Pollution – urban and regional; Troposphere - composition and chemistry)

Correspondence to: V. E. Cachorro
(chiqui@baraja.opt.cie.uva.es)

1 Introduction

The detection and characterization of desert dust aerosols on a global scale and hence in different areas of the world is necessary to evaluate dust aerosol radiative forcing (Tegen and Lacis, 1996; Tegen et al., 1996; Miller and Tegen 1998). Its influence, along with other types of aerosols, is considered to be crucially important, even though its magnitude is still highly uncertain (Shine and Forster, 1999; Haywood and Boucher, 2000; Haywood et al., 2001). Desert dust events have been widely studied in recent years using a variety of measurements, including those from ground-based, aircraft and satellite sensors (Karyampudy et al., 1999; Husar et al., 2001; Díaz et al., 2000; Ginoux et al., 2001; Kinne et al., 2001). Such data are valuable for assessing various available desert dust models (Longtin et al., 1988; D'Almeida et al., 1991). It is also becoming increasingly clear from recent observations that these models must be adapted to account for the physical and chemical modification of the dust particles as they are transported over long distances from their source regions.

In this paper, we focus on desert dust outbreaks originating in North Africa (Sahara, Sahel) that reach the Iberian Peninsula. In Spain, the so-called *red rain* (corresponding to wet deposition of desert dust) has been used as an indication of the frequency and extent of these desert dust outbreaks (Avila et al., 1997). Recent studies concerning African dust outbreaks reaching the Iberian Peninsula are reported using back-trajectory air masses. These studies evaluate the influence on ground particle mass concentration measurements of Air Quality networks, resulting from desert dust outbreaks (Rodriguez et al., 2001; Querol et al., 2002a, b; Sanchez de la Campa, 2002). The data for PM10 (particle diameters less than 10 μm) concentration are of particular interest

Published by Copernicus GmbH on behalf of the European Geosciences Union.

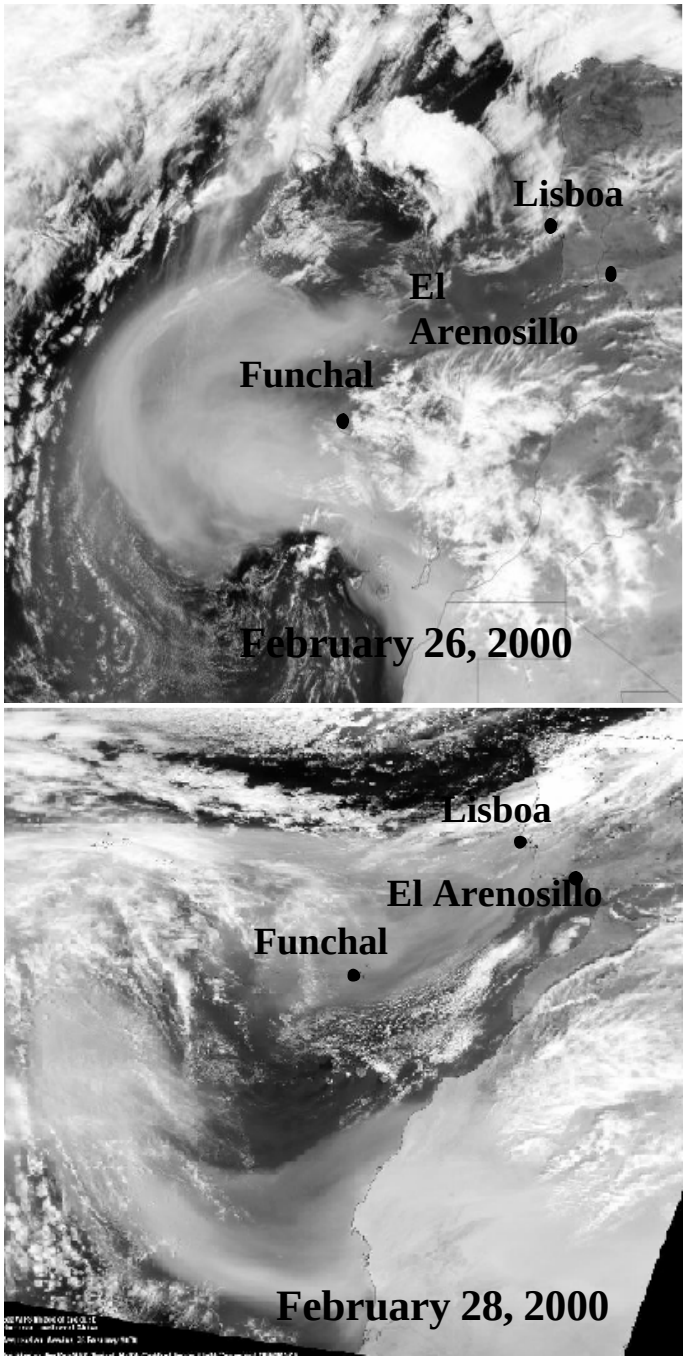

Fig. 1. (a) SeaWiFS sensor image for 26 February of year 2000, showing a Saharan desert dust outbreak spreading out over the Atlantic Ocean and southwestern region of the Iberian Peninsula; **(b)** image for 28 February where the dust plume reaches the Iberian Peninsula from the southwest.

because the recent European Union Directive 1999/30/CE on Air Quality established PM10 limit values, which are frequently exceeded in rural areas of Spain and southern Europe due to the occurrence of desert dust outbreaks (Artiñano, 2001; Querol et al., 2002a, b) thereby making attainment of this directive difficult.

Outbreaks of desert dust plumes, similar to those observed over the Iberian Peninsula, have been analysed over the Mediterranean Sea (Prospero, 1996; Guerzoni et al., 1997; Moulin et al., 1997a), The Canary Islands (Bergametti et al., 1989; Smirnov et al., 1998; Díaz et al., 2001) and the Atlantic Ocean (Prospero, 1999; Moulin et al., 1997b). Pinker

et al. (2001) has also analyzed a strong outbreak which occurred between the end of January and the beginning of February 2000 over the western sub-Sahel, which has many similarities with our first case study presented in this paper.

The opportunity to follow African desert dust events that reach the Atlantic Ocean and the Atlantic coast of the Iberian Peninsula from multiple stations is not very typical. In this study, available aerosol measurements at three different sites of Funchal on the Madeira Island, Lisboa on the Atlantic coast of Portugal, and El Arenosillo (Huelva) in the southwest coastal area of Spain, allows a detailed analysis of two desert dust outbreaks observed during 2000.

The aim of this work is to detect and determine optical and physical properties of desert dust aerosols over the southwestern coast of the Iberian Peninsula in terms of AOD and Ångström coefficient, α (if available), together with complementary data, such as back-trajectory analysis, satellite images and weather maps. Available AOD data at the three different stations have allowed the study of two different desert dust events and a detailed analysis of size distribution and other microphysical and radiative parameters (thanks to data from a Cimel photometer at one site).

The structure of the paper is as follows: Sect. 2 gives details of the measurement sites and instruments. Section 3 briefly describes the methodology and support data. Section 4 summarizes the measurements and results. The first part focuses on the detection and identification of desert dust episodes and the latter parts are focused on a more detailed description of the two selected episodes – a strong winter episode and a somewhat weaker summer episode.

2 Measurement sites and instruments

The station at El Arenosillo (37.1 N, 6.7 W, 10 m ASL and #213) in Huelva (Spain), is part of Instituto Nacional de Técnica Aeroespacial (INTA). The stations at Lisboa (38.77 N, 9.15 W, 105 m ASL and #082) and Funchal (32.64 N, 16.89 W, 58 m ASL, and #287) on Madeira Island belong to Instituto de Meteorologia of Portugal. (The station numbers are those designated by the WMO network to track ozone atmospheric content.) These three stations are very good sites for solar radiation measurements and aerosol studies due to their geographical location with maritime background aerosols. Lisboa also has a significant urban aerosol component. Continental sources can have an important effect at El Arenosillo and Lisboa, but desert dust outbreaks, as we will show later, seem to have a major influence at the three sites. Figure 1 shows the location of the three stations (black points) on two SeaWIFS images, where one of the two selected desert dust storm case studies is depicted.

In this work we focus particularly on the application of Brewer spectroradiometer measurements to derive AOD data. The Brewer instruments were designed for ozone monitoring (Kerr, 1981) using five wavelengths (306.6, 310.1, 313.5, 316.8, 320.1 nm, respectively; some differences exit between instruments and models) and require 3 min per wavelength scan. They also were designed to measure the spectral UV global irradiances from 286.5–363 nm (depending on the model, single or double monochromator) with a step scan of 0.5 nm and with a nominal HWHM (Half-Width at Half Maximum) of 0.62 nm. Direct and global irradiance measurements have different fore-optics in the Brewer system (a rotating prism and a cosine receptor, respectively), each of which required different calibration procedures. The FOV (Field Of View) of the instrument is controlled by an iris, which can be set to about 2° (used regularly for the direct sun measurements) and 10°. Five neutral density filters with increasing attenuation (up to about a total of 10^{-5}) can be inserted into the beam path to protect the photomultiplier (the detection system) from overexposure to sunlight. These filters increased the difficulty of the calibration procedure.

The three Brewer systems follow the requirements established by the Brewer WMO network and are calibrated periodically according to NIST standards against the Brewer Reference Travelling Standard #17 operated by the International Ozone Services (IOS). Details about the Brewer instrument characteristics, performance and maintenance may be found at (http://www.woudc.org/).

UV radiation measurements, made by YES pyranometers (1-min resolution) at El Arenosillo and Lisboa, were used in this work as support data to detect the presence of clouds. Details of these instruments, measurement and calibration procedures are found elsewhere (Yankee user guide, 1996; Vilaplana et al., 2002; Vilaplana, 2004). These measurements were also important for other research studies related to the decrease in UV radiation during high turbidity episodes, such as those due to desert dust outbreaks.

An AERONET (AErosol Robotic Network, (Holben et al., 1998)) Cimel sun-photometer (in operation at El Arenosillo station since February 2000) allows the determination of AOD and additional aerosol properties. El Arenosillo's Cimel photometer is a polarized instrument model CE318-2 with 8 filters, where the filters at wavelengths of 440, 670, 870, and 1020 nm, respectively, are used for aerosol studies. AOD values at these 4 wavelengths and the derived Ångström exponent, α, are obtained as primary aerosol parameters. With the addition of sky radiance measurements and inversion algorithm methodology, other aerosol properties are determined, such as volume size distributions, refractive index, single scattering albedo, etc. For details of this instrument, the measurements and derived aerosol parameters, see Holben et al. (1998), Eck et al. (1999), Smirnov et al. (2000) and Dubovik et al. (2000, 2002a, b).

Table 1. Available measurements (X) in each station for the two considered desert dust events. Columns are from left to right: AOD from Brewer, TOMS aerosol index, AOD from Cimel, effective UV irradiance, back trajectories computation and cloud screening using UV measurements and Meteosat data. X(*) denote only Meteosat data.

July–August Event	AOD Brewer	A.I. TOMS	AOD Cimel	UV YES	Backtraj.	Cloud Screening
Lisboa	X	X	–	X	X	X
Funchal	X	X	-		X	X(*)
Arenosillo	X	X	X	X	X	X
March Event						
Lisboa	–	X	–	X	X	X
Funchal	X	X	–		X	X(*)
Arenosillo	X	X	X	X	X	X

3 Methods and supporting data

Multi-year data sets (meteorological variables, radiation data, etc.) are monitored at the three sites using different instruments. These atmospheric variables can be used to detect and evaluate desert dust episodes. Surface AOD is certainly an important parameter for desert dust detection. Examination of the AOD series shows the relatively high frequency of desert dust outbreaks over the three sites. However, a reliable criterion needs to be established to clearly identify desert dust events. Indeed, for weak desert dust outbreaks, AOD is not sufficient and complementary information is generally necessary. Thus, back-trajectory analysis, synoptic weather maps, satellite images and other parameters, such as the aerosol index (A.I.), are used to evaluate and characterize the desert dust aerosols transported over the study region. Table 1 summarizes the type of data used for the two selected case studies.

3.1 Aerosol optical depth and Ångström exponent α

AOD is a key aerosol parameter, defining the level of turbidity in the atmosphere. Indeed, AOD is a good indicator of desert dust outbreaks which generate high atmospheric turbidity (Pinker et al., 2001; Eck et al., 1999; Dubovik et al., 2002a).

In this work we focus particularly on the application of Brewer spectroradiometer measurements to derive AOD at El Arenosillo, Lisboa and Funchal sites. As is well known, the Brewer instruments are currently used for the ozone content retrieval (Kerr et al., 1981), but recently, research efforts have addressed the use of Brewer measurements for AOD retrieval (Carvalho and Henriquez, 2000; Gröbner et al., 2001, Kirchoff et al., 2001; Kerr, 2002; Marenco et al., 2002; Cachorro et al., 2003; Kazadzis et al., 2005). Although not systematic and operational, AOD monitoring by Brewers system has been conducted recently at different sites (Kerr, 2002; Jaroslawsky et al., 2003; Cheymol and De Backer, 2003; Gröbner and Meleti, 2004; Kazadzis et al., 2005). The method we have followed for AOD determination using Brewer measurements is based on the work of Carvalho and Henriquez (2000) using the routine DS data. In addition, the values determined in this work have also been assessed with those calculated following the procedure used in Gröbner et al. (2001).

Errors associated with Brewer measurements are difficult and laborious to evaluate (Kerr 2002; Gröbner and Meleti, 2004; Arola and Koskela, 2004; Kazadzis et al., 2005), because ozone, AOD and global UV irradiance follow different calibration procedures and retrieval methods. Therefore, various methods have been developed for this determination, where the main problem is how to obtain direct irradiance for applying the Beer law (for details, see the recent work of Kazadzis et al., 2005). Absolute error values of 0.07 are estimated in Arola and Koskela (2004) and Kazadzis et al. (2005) for Brewer AOD values. Thus, taking 0.3 as a representative and realistic value of the AOD in the UV, we estimate a relative error of $\sim$25%.

With respect to the AOD derived by the Cimel sunphotometer, we used data provided by the AERONET procedure. An error of 0.02 is estimated for AOD sun-photometer data (Holben et al., 1998; Eck et al., 1999). We also considered values of α (Ångström exponent), as it adds valuable information, together with AOD for desert dust detection. Here we use the Ångström formula AOD=$\beta\lambda^{-\alpha}$, where λ is the wavelength (in μm), α is the Ångström exponent, and β is related to the concentration of aerosols (β is also the AOD at λ=1 μm). The Ångström exponent α is derived from a log-log fit of the AOD data using three wavelengths (440, 670 and 870 nm, respectively), according to the AERONET procedure (Eck et al., 1999; Holben et al., 2001). This procedure uses quantitative information about the spectral curvature of the AOD, which, in turn, is related to the particle size distribution.. Values of α>1.0 are indicative of size distributions dominated by fine particles, while 0<α<0.8 tend to be

dominated by large particles (Eck et al., 1999; Holben et al., 2001; Dubovik et al., 2002a).

AOD and α are the primary key parameters in defining the climatology of aerosols in a given region (Hess et al., 1998; Holben et al., 2001; Dubovik et al., 2002a). Desert aerosols (Longtin et al., 1988; D'Almeida et al., 1991) are characterized by high AOD values and low α values, resulting from an abundance of large particles. Dubovik et al. (2002a) defines a range of climatological α values for desert aerosols at four representative sites; i.e.: ($-0.1 \leq \alpha \leq 0.7$ at Cape Verde and ($0 \leq \alpha \leq 1.55$ at Lanai). However, the observed wide range of values (including negative values) makes this parameter only a good indicator, but not a definite one. A more robust characterization of desert aerosols is obtained when size distribution and optical properties are combined. Radiance data, together with Cimel AOD data, allow the application of the inversion algorithm to retrieve these properties.

3.2 Satellite images

Desert dust events can also be detected and quantified by means of satellite observations (e.g. Fig. 1). Qualitative and quantitative aerosol information is available from spaceborne sensors, such as SeaWIFS (Wang et al., 1999); MODIS (Tanré et al., 1997), AVHRR-NOAA (Stowe et al., 1997), METEOSAT (Moulin et al., 1997a); TOMS (Torres et al., 1999).

Although the extraction of physical aerosol parameters from satellite sensors is difficult (Stowe et al., 1997; Tanré et al, 1997), retrieval methods are being improved and evaluated. Usually, satellite retrieval results are generally validated using ground-based measurements, but in this study they are used as complementary information to ground-based data and for a qualitative visualization of desert dust events.

3.3 Cloud screening methodology

Desert dust episodes are frequently accompanied by clouds and rainfall. Radiometric systems are very sensitive to cloud coverage, with global radiation being a useful tool to detect the presence of clouds. AOD measurements are also useful for cloud detection, as demonstrated by the Cimel AOD data retrieval algorithm (Smirnov et al., 2000). The Brewer AOD data must also be examined for possible cloud contamination. Satellite images, such as those of Meteosat and SeaWIFS, serve as complementary information in that regard. Examination of the Meteosat infrared images over the study region, we observe qualitatively that the February-March event is certainly affected by cloud coverage. For the July-August episode, no clouds appear in the IR images.

The Cimel measurements for El Arenosillo are processed using a cloud screening algorithm, following a criterion based on the variability of AOD during triads of measurements taken for each datum (Smirnov et al., 2000). If this variability is higher than a certain level, the measurement is discarded as cloud affected. Data at this level of screening (level 1.5 in the AERONET database) are those used here. No specific screening algorithm is applied to the Brewer AOD data, other than discarding those AOD data as determined by the Cimel criterion at the El Arenosillo station.

In general, we have used UV global radiation data from the YES UV-pyranometer to detect the presence of clouds and to discard any Brewer AOD data affected by them. The procedure consists of an evaluation of the time interval where the shape of the global radiation curve deviates from a cloud-free day radiation by more than 10%. The application of this screening criterion to the Brewer AOD data is consistent with the AERONET cloud screening technique used in the analysis of the Cimel AOD data for the February–March episode at El Arenosillo.

Unfortunately, no UV radiation data were available at Funchal. Although only qualitative and not very efficient, we inspected Meteosat infrared images as a means for discarding Brewer AOD data contaminated by clouds. During the first case study, the highest AOD days also coincided with the highest A.I. and clouds, making it difficult to describe the evolution of this episode in any quantitative manner.

3.4 Back-trajectories and synoptic weather maps

Back-trajectory analysis was also carried out as complementary information for dust events. Back-trajectories were computed with the HYSPLIT (HYbrid Single-Particle Lagrangian Integrated Trajectory) model, a program developed by NOAA (Draxler, 1996; Draxler and Hess, 1997, 1998), to study the movement of a particle within an air mass. In this study, we used the FNL database, archived by NOAA (National Oceanic and Atmospheric Administration; www.arl.noaa.gov/ss/transport/archives.html). The output of the model is a set of points (one per hour) that permits the tracking of the positions of the air mass in the atmosphere in latitude, longitude and height, according to the vertical velocity field. In order to minimize the usual errors of atmospheric dynamic computations, only back-trajectories with a maximum duration of five days were considered (Stunder, 1996; Stohl, 1998; Derwent et al., 1998; Cape et al., 2000).

Daily back-trajectories for the year 2000 were computed for air masses arriving at 12:00 GMT at El Arenosillo (at Lisboa and Funchal, only those days around the two selected desert episodes were calculated) for final site altitudes of 3000, 2000 and 1000 m, respectively. The highest levels are particularly suited for desert aerosol assessment (Vergaz, 2001; Rodriguez et al., 2001; Querol et al., 2002a, b). From an inspection of these trajectories, we assign those arriving from North Africa as desert dust episodes, which allows an evaluation of the episodes and number of dusty days during 2000 (Vergaz, 2001; Vergaz et al., 2005).

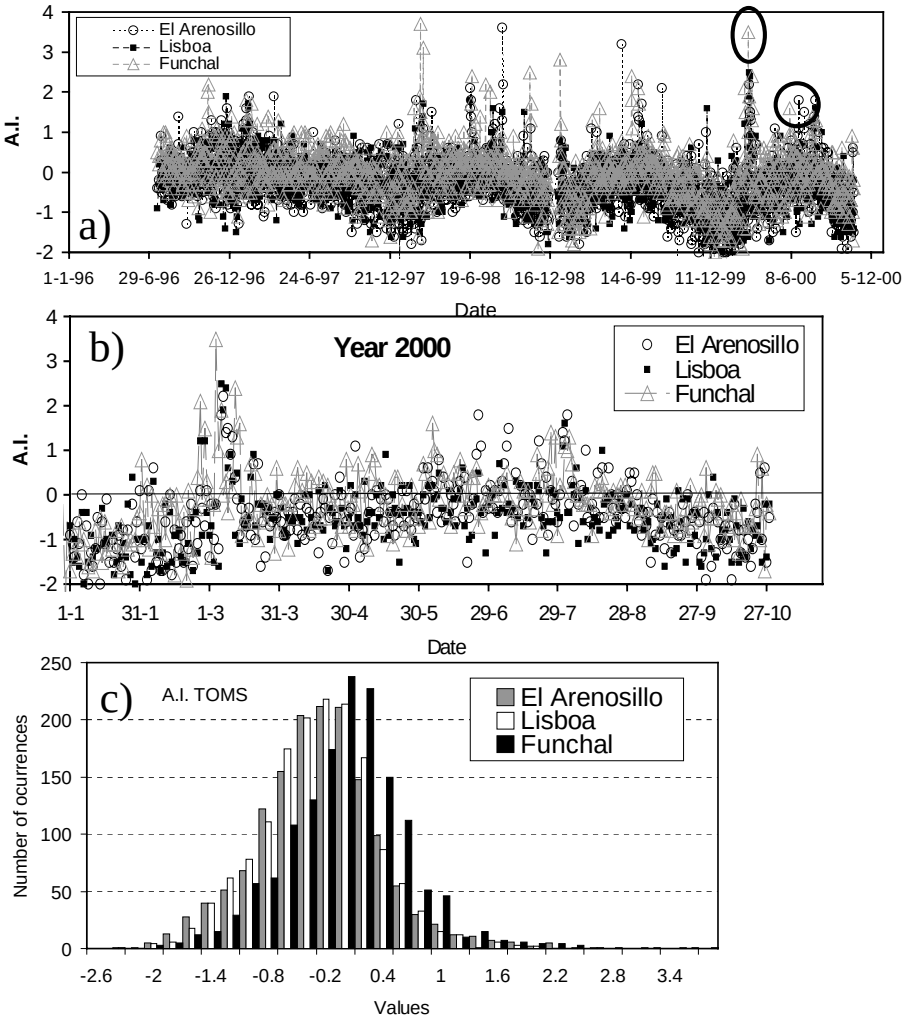

Fig. 2. (a) Evolution of TOMS' Aerosol Index from July 1995 to December 2000 for the three stations: Funchal, Lisboa and El Arenosillo. **(b)** The same for year 2000. **(c)** Frequency distribution function of AI values over the three stations.

Additionally, synoptic weather maps were obtained from the NOAA FLN data set (http://www.arl.noaa.gov/ready/amet.html) at the 700 hPa, 850 hPa and surface levels as complementary information for the two case studies.

3.5 TOMS Aerosol Index

A frequently used aerosol parameter to monitor desert dust outbreaks is the TOMS (Total Ozone Mapper Spectrometer on the Earth-Probe satellite) Aerosol Index (A.I.) (Herman et al., 1997; Cakmur et al., 2001; McPeters et al., 1998). The TOMS A.I. is based on the backscattered radiance measured in the 331 and 360 nm channels and is indicative of the aerosol content over the study area. If the A.I. is large and positive, absorbing aerosols and high turbidity are present in the atmosphere; if it is negative, the aerosol is nonabsorbing (Hsu, 1999). Also, A.I. is insensitive to aerosols below 2 km. Moreover, weakly absorbing aerosols are difficult to detect. Nevertheless, we use A.I. as one of our indicators of desert dust outbreaks over the three sites.

4 Results and discussion

4.1 Detection and evaluation of desert dust events in year 2000

The TOMS A.I. time series (Fig. 2a) from mid-1996 to the end of 2000 suggests an annual cycle, with a winter minimum which seems to have decreased slightly. We can also compute a mean A.I. and standard deviation for each of the three stations. The data set, however, is too short to establish any meaninful trend. Figure 2b shows A.I. values for 2000 only, where the strong events recorded for each station are easily detected. Figure 2c shows the number of occurrences

Table 2. Detected desert dust outbreaks at Funchal, Lisboa and El Arenosillo during year 2000 according AI values threshold.

Funchal	Lisboa	El Arenosillo
26–28 Feb	26–28 Feb	
4–6 Mar and 11–14 Mar	6–8 Mar	6–11 Mar
		3 May
5 June		
		25–26 Jun
		7–8 Jul
		21 Jul
26 Jul–3 Aug	31 Jul–2 Aug	31 July–2 Aug

of A.I. values for each station. Funchal registered the highest number of occurrences, while Lisboa and El Arenosillo have distributions which are quite similar to each other.

After some experimentation, we found that a threshold A.I. value equal to the mean plus twice the standard deviation (STD) is sufficient to detect most desert dust events. The threshold values at the 3 sites are 1, 0.9. and 1.3 for El Arenosillo (mean = –0.29, STD = 0.66), Lisboa (–0.31, 0.6), and Funchal (0.05, 0.66), respectively. Applying these values the 2000 time series resulted in 5 episodes at Funchal (with a total of 19 days), 3 in Lisboa (9 days) and 6 in El Arenosillo (15 days). These data are summarized in Table 2.

We selected for case studies only those events for which the A.I. exceeded the threshold at all three stations simultaneously. Only two such episodes were selected: a strong episode in early March (4–14 March) and another at the end of July/beginning of August. A third event was a common episode to Funchal and Lisboa on 26–28 February, but not to El Arenosillo, and thus was not selected.

The A.I. appears to be a useful parameter for detecting strong desert dust events, but not moderate or weak episodes. This will be discussed later in the context of evaluations of the El Arenosillo data. This is also confirmed by the poor correlation between A.I. and mean daily Cimel AOD data at 440 nm over the region (see Fig. 3), where only a qualitative correlation appears for AOD greater than 0.4 and A.I. greater than 1.

To detect and evaluate desert dust outbreaks over El Arenosillo during 2000, we have examined the Cimel-derived AOD time series (Fig. 4). Several episodes of high turbidity can be observed, many of which could be considered the result of desert dust outbreaks. Although the large AOD values can be assumed to be a result of desert dust events when compared to normal atmospheric conditions, we need to define a threshold for AOD values which provides an unambiguous identification of desert dust episodes. From the 2000 AOD time series (at 440 nm) and with a similar method

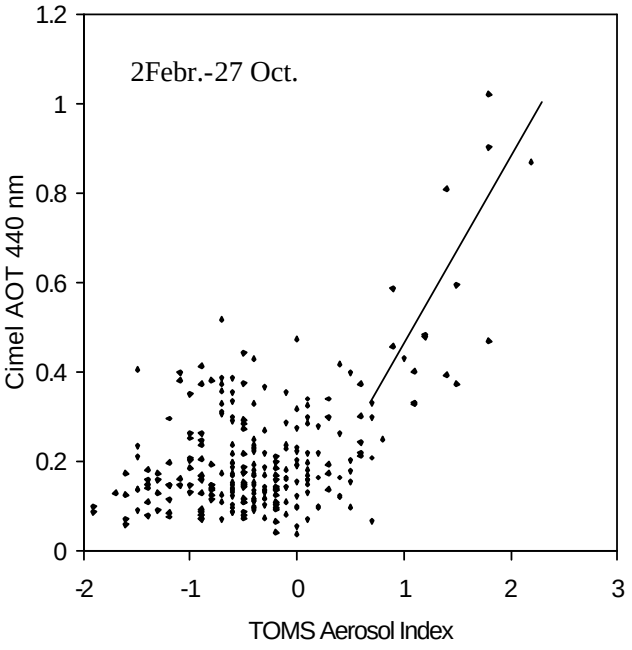

Fig. 3. AOD at 440 nm versus and TOMS A.I. at El Arenosillo. A qualitative straight line is drawn for high A.I. and AOD values.

used for A.I., we compute a mean and standard deviation 0.19 and 0.14; respectively, to estimate a threshold of 0.3. However, since AOD can be large for non-dust conditions, it is necessary to include the wavelength information provided by the Ångström exponent, α, to remove the nondust cases. Generally, values of α greater than 1 are associated with fine particles, while those less than 1 have a significant contribution from coarse (dust) particles. As can be seen in Fig. 4 a strong anti-correlation exists between AOD values and α during high turbidity episodes, i.e. when AOD increases, α decreases, with α approaching values near zero. The average α is 0.8, with a STD = 0.4. We adopt a threshold of 1.0 as the maximum value for α for a dust episode. With the AOD and α criteria, we have 14 events with a total of 27 days.

We can also evaluate desert dust episodes by means of back-trajectory analysis, taking the levels there and assigning those with a clear origin over a geographical sector covering North Africa (for details, see Vergaz, 2001; Vergaz et al., 2005). For 2000 (not including January) at El Arenosillo, there were 21 desert events with a total of 60 days.

Comparing the event selection results between these two methods indicates that the threshold values using AOD and α are perhaps too restrictive. We notice that the days corresponding to the beginning and the end of the episode are not accounted for and only the "central" days are included in the automatic filtering of the Cimel data. Using a lower threshold AOD value of 0.26 and $\alpha \leq 1$, we find 18 events with a total of 39 days. These events indicated in Fig. 4, where single day events (3, 5, 8, 11, 13, 15, 16, 17, 18) are denoted with

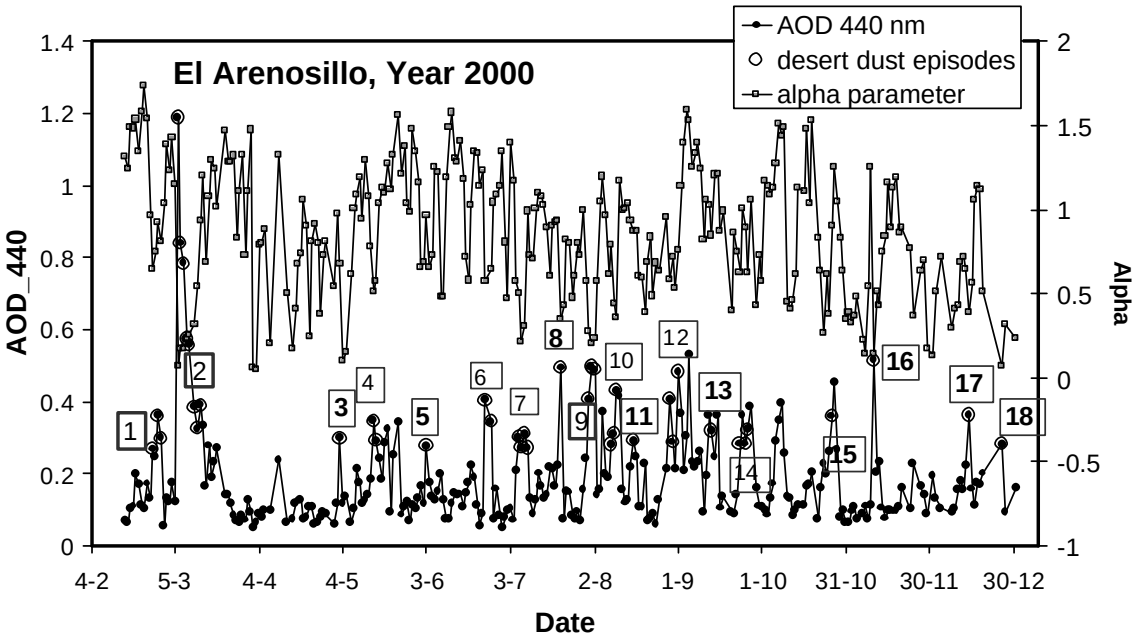

Fig. 4. Average daily values for AOD at 440 nm and the α parameter evaluated by Cimel AERONET during year 2000 at El Arenosillo. The numbered episodes correspond to those determined by manual inspection.

a bold number, while events 1, 2 and 9 (marked with a bold square) are the selected case studies. Although the number of events and days has increased and agrees better with the air mass trajectory method, the difference between the two methods remains high.

As a consequence of the different results from the two methods described above, we decided to perform a joint examination of the Cimel AOD database and the air mass trajectories. We have taken all available data (not the filtered, average daily values) of the AOD-α database (with the latter threshold AOD and α values) and the corresponding daily back-trajectories, with the analyst deciding whether or not to include a particular day as belonging to a given dust episode. In this analysis, 18 events with a total of 72 days were obtained.

The coincidence between the number of episodes from the joint examination and automatic filtering of the Cimel data indicates that the thresholds chosen for the Cimel data were satisfactory. The large difference between the number of days may be explained by the uncertainties in selecting the beginning or ending of an episode, which were not taken account previously.

We conclude from the foregoing discussion that a truly automated algorithm for selecting dust events is not yet possible without some analyst intervention. Nevertheless, we have shown that through suitable selection of threshold values of aerosol parameters, such as A.I., AOD, and α, that reasonable event identification is possible. It is also clear that detailed analysis of data from several years is needed to refine the selection criteria. We note that the same variability in desert dust events occurs every year over the Iberian Peninsula (Rodriguez et al., 2001).

4.2 Case study 1: winter desert dust episode

As mentioned above, this case study, February – March, is characterized by great intensity and long duration. Figure 4 shows that this episode can be considered as composed of two desert dust events separated by four days with low AOD (below 0.2). However, due to the strong intensity and the great spatial extent of the associated dust plume, we analyse them together, as part of continuous meteorological conditions over the Saharan region. Furthermore, the episode is highly contaminated by clouds with rainy weather conditions, making its characterization by radiometric data complicated.

In Fig. 5, a plot of the Cimel AOD (440 nm), together with the α coefficient at El Arenosillo, documents the main features of the event. On 25 February the AOD is $\sim$0.2 exhibits large variability compared to normal conditions for low AOD values. The Ångström α coefficient decreases from about 1.2 to 0.6, suggesting the presence of dust at the end of the day. During 26 February (see Fig. 1a) the dust is well established and AOD increases to 0.5 on 28 February (see SeaWIFS image in Fig. 1b) and decreases to 0.4 on 29 February. AOD decreases to normal values in the following days. The α coefficient decreases during the AOD increase and vice versa, leading to a good anticorrelation during the episode 25–29 February. However, it must emphasized that AOD and α are highly variable during the entire period.

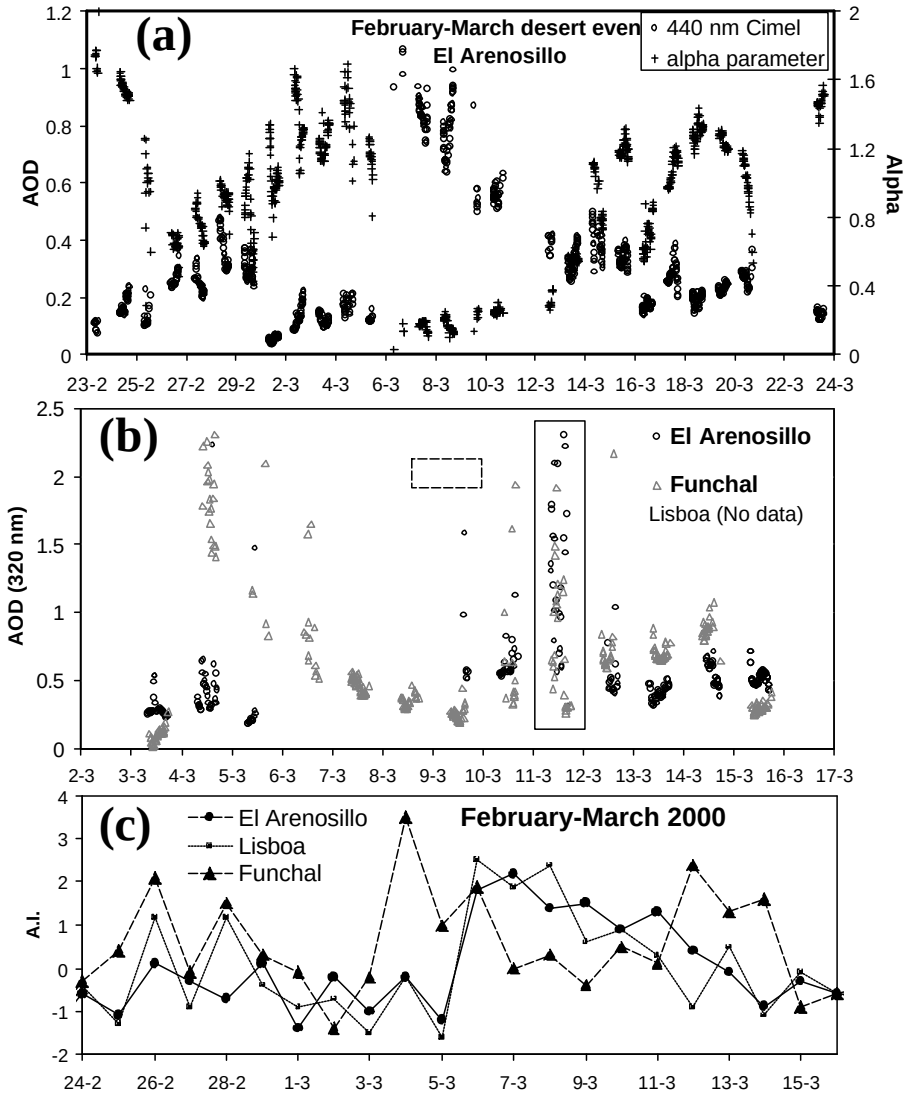

Fig. 5. AOD at 440 nm and α evolution at El Arenosillo station for the February–March desert dust event. **(b)** AOD Brewer data at 320 nm for the same event at the three stations. **(c)** same as b) but for A.I. values.

The second part of this episode began on 6 March, according to the Cimel data. The AOD reaches a maximum value of ~ 1, while on 5 March it is only ~ 0.2. There were no Cimel data available during the afternoon on 5 March and most of 6 March, because of clouds and rain (corroborated by UV radiation data, SeaWIFS and Meteosat images, not shown). Simultaneously, the α values decrease from about 1 to near 0, clearly indicating a desert dust event. The end of this event is not to define, because dust remains several days after the maximum, with AOD quite slowly. Based on the nearly normal AOD values, March 15 appears to be a reasonable date for the end of the episode.

Figure 5b illustrates the Brewer AOD (320 nm) time series at Funchal and El Arenosillo from 3 March. Since Brewer data were not available in February, the first part of the event cannot be displayed. No Brewer data were available at Lisboa during the entire episode. Brewer AOD data and A.I. values in Fig. 5c are analyzed together for all three stations. At El Arenosillo, despite a limited number of measurements, the Brewer AOD data exhibit the same features as the Cimel AOD data. The highest A.I. (greater than 1 from 5–9 March) are observed in accordance with AOD.

At Funchal, the event shows a slightly different temporal behaviour than at the other two sites. Although the first part of the event also arrives on 25 February (24 February has a low A.I.), with the highest A.I. values on 26 and 28 February, the second part in March shows a different evolution. It

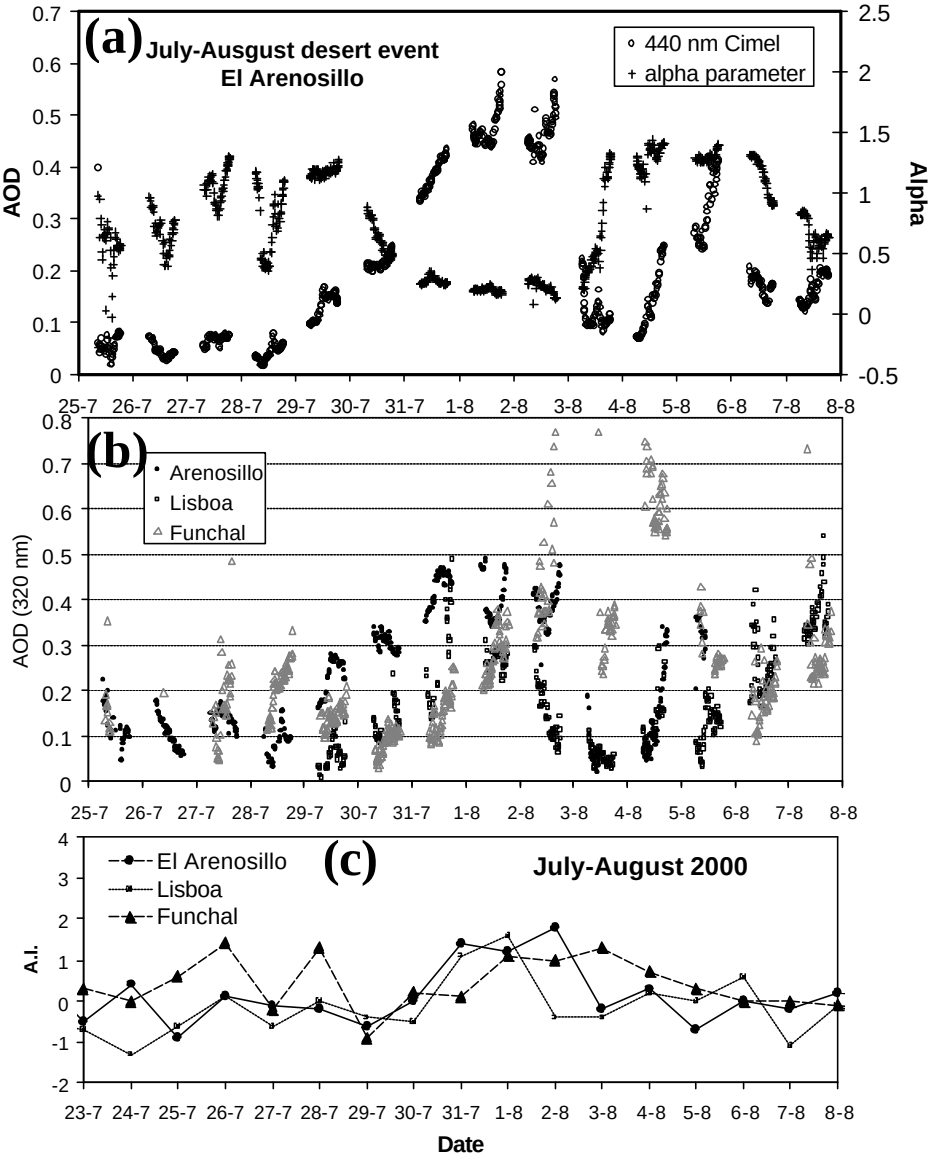

Fig. 6. AOD at 440 nm and α evolution at El Arenosillo station for the July-August desert dust event. **(b)** AOD Brewer data at 320 nm for the same event at the three stations. **(c)** same as (b) but for A.I. values.

begins with the arrival of a large plume on 4 March (two days earlier than at El Arenosillo), with a maximum of A.I. of $\sim$ 3.5 and high AOD values. We note that the minimum A.I. value of 1.5 occurred on 2 March. A.I. values remain high on 5 and 6 March. A second A.I. maximum is observed on days 12–14 March. The days between 6 and 12 March, as well as at the end of the episode, show high variability. It is likely that much of this variability may be a result of cloud contamination, as mentioned earlier, and thus made it difficult to assess the true AOD at Funchal.

4.3 Case study 2: summer event

4.3.1 General description: AOD and alpha values

During the summer event (July–August 2000), a better, more quantitative characterization was possible due to noncloudy conditions. Figure 6 documents the AOD and A.I. values for this event. The AOD (440 nm) at El Arenosillo (Fig. 6a) clearly shows that this episode is less intense compared to the winter episode. AOD begins to increase in the afternoon of 29 July, but does not exceed values greater than 0.2 (a typical value in summer). As α is stable at $\sim$ 1.3, it suggests that desert dust aerosols are not yet present.

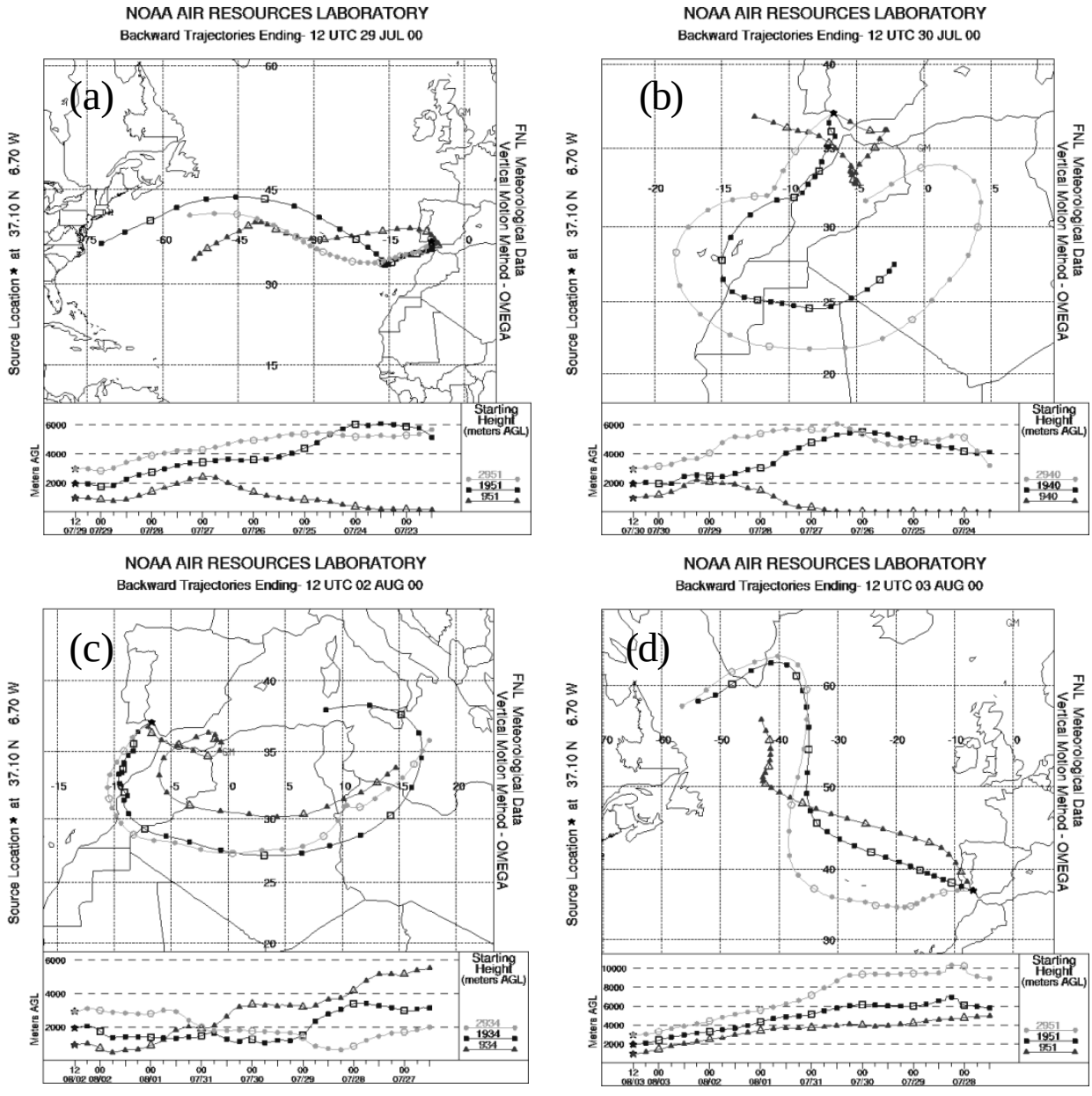

Fig. 7. The three levels of back-trajectories at 12:00 UTC at El Arenosillo on 29 and 30 July and 2 and 3 August, evaluated by the NOAA HYSPLIT.

On 30 July, the AOD values are still not large, ∼0.22–0.28, but α is decreasing, which suggests that the dust event is beginning to establish (also confirmed by back-trajectories, as discussed below). AOD values reach a maximum of 0.6 on 1 August and remain at similar values on 2 August. Values drop considerably during 3 August, but still exhibit dusty characteristics. On subsequent days (4–5 August), AOD again increases, but with larger values of α, which probably represents a mix of aerosol types. AOD and α show the expected anti-correlation during the event, with α decreasing from ∼1.3 on 29 July to ∼0.1 on 1 and 2 August, when AOD is highest. Using the Cimel AOD-α threshold criteria, the automatic dust event algorithm includes 31 July and 1 and 2August, but not 30 July and 3 August, which are included with analyst intervention.

Brewer AOD data (Fig. 6b) increases smoothly at El Arenosillo and Lisboa (with lower values at Lisboa) until the event is well established at both, between 31 July and 2 August. Similar to the Cimel AOD, the Brewer AOD decreases sharply on 3 August, where it would seem that the event has ended, despite the high and variable AOD values on 4–5 August.

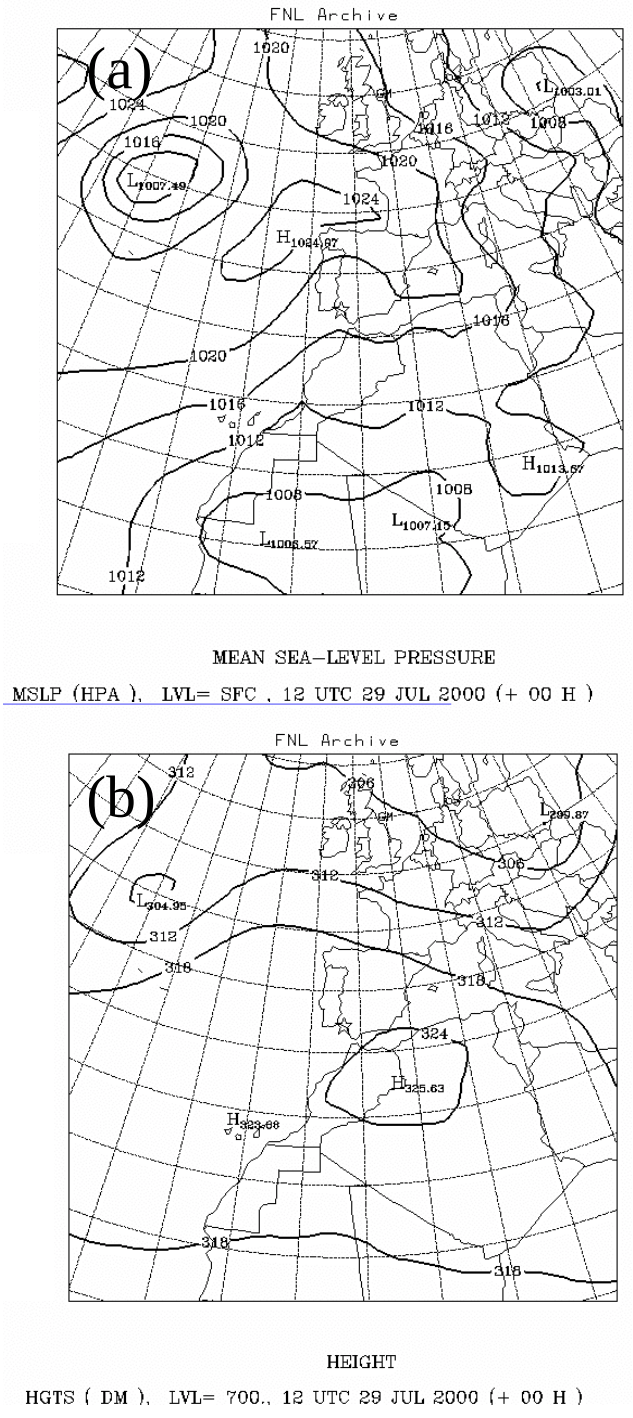

Fig. 8. Synoptic weather conditions in the study area on 29 July, given by the surface pressure, and 700 mb maps generated by the NOAA FNL archive.

Inspection of back-trajectories at El Arenosillo (Fig. 7) shows that the 29 July (12:00 UTC) air mass trajectories at all three levels come from the Atlantic, but on 30 July they arrive from North Africa, suggesting that the event probably arrived during the night. The back-trajectory at 1000 m. is more complex compared with the other two levels (2000 and 3000 m respectively). The latter have a clear Africa origin, while the former indicates re-circulation, with the air mass coming from the Mediterranean area, but having its origin in North Africa. Back-trajectories on 2 August show a clear African origin, while on 3 August the air masses come from the West Atlantic, corroborating earlier conclusions from the Cimel-Brewer data about the end of the episode.

The event at Funchal exhibited some differences compared with the other sites, namely with respect to intensity and variability. It began on July 26, as indicated from back-trajectories (not shown) and was fully established on 1–4 August, with AOD values reaching a maximum of $\sim$ 0.8 on 2 August. The event persisted through 7 August, with decreasing, but relatively high AOD values and with α values consistent with desert dust. Interestingly, back-trajectories on 6 August (not shown) indicated a North Atlantic origin, suggesting that the dust plume may have undergone some re-circulation over the ocean.

It is interesting to note that the Brewer AOD at 320 nm is lower than that of the Cimel AOD at 440 nm during the maximum of the summer event (31 July–2 August), in contrast to the previous days, when background conditions prevail. This behaviour in the UV is also consistent with the flat spectral dependence of desert aerosols in the visible.

Figure 6 shows a clear correspondence between dust-related AOD and positive A.I. values at each station. The exception appears to be at Funchal on 26 and 28 July, where A.I. values greater than 1 are observed, while the Brewer AOD data are less than 0.3. Also, we have inspected the daily TOMS A.I. contour maps of the dust plumes of over the extended region around the three sites from 28 July to 4 August. These maps show that the intensity of the dust episode is greatly diminished by the time it reaches the measurement sites, compared to other locations closer to the dust sources. It is likely that inhomogeneities in the dust plume, as it is transported out over the Atlantic and back toward the Iberian Peninsula, accounts for the variability observed from site to site.

The synoptic weather conditions over the study region on 29 August are shown in Fig. 8. These appear to be the most frequent type of weather situations for dust transport over Spain during the summer months. The surface pressure map shows a thermal low over the North African Sahara as a result of the intense surface heating. An upper level high induces a convective system which pumps dust to high altitudes (3000–5000 m) leading to a large dust charge. If the high moves eastward, the air masses move from south to north, covering a wide area of Mediterranean, including the Gulf of Cadiz and the Iberian Peninsula, transporting the dust-laden layers. Most summer events follow this pattern (Rodriguez et al., 2001).

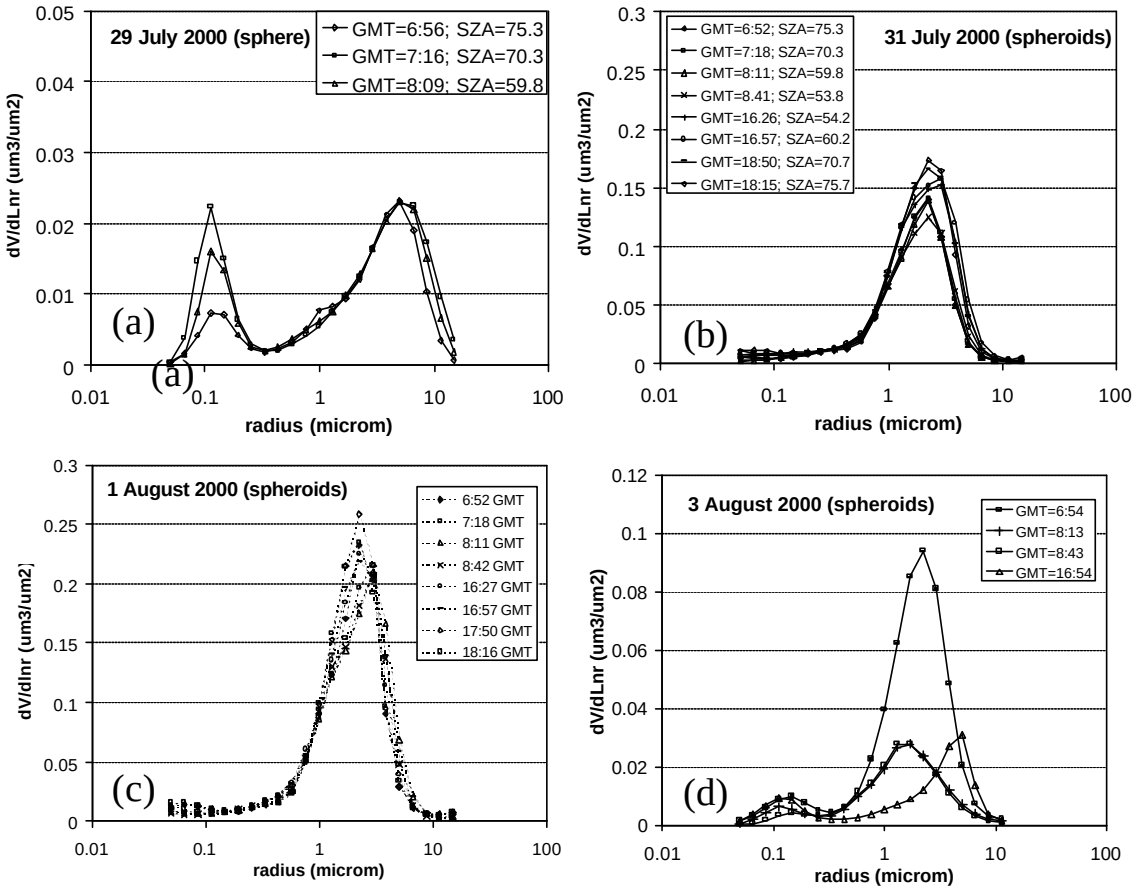

Fig. 9. Volume particle size distribution functions at representative days before, during and after the desert dust event of July–August at El Arenosillo, obtained by inversion of AOD and sky radiance measurements by the CIMEL instrument (AERONET inversion protocol).

4.3.2 Aerosol particle size distributions and radiative parameters

Relevant aerosol properties for this study are the particle size distribution, the asymmetry parameter g, refractive index and single scattering albedo SSA, which are obtained by the inversion method developed by Dubovik and King (2000) and Dubovik et al. (2000). The values and evolution of these aerosol parameters obtained from the CIMEL measurements at El Arenosillo provides valuable information about the dust aerosols over this region.

The inversion method uses AOD values and sky radiance measurements at all scattering angles and assumes that the Mie theory applies for spherical particles. The method is only applicable for clear-sky (noncloud) conditions. A check for nonsphericity was necessary for these data because of the appearance of an unusually large accumulation mode in the retrieval when using the spherical model. This artifact of the algorithm was resolved by Dubovik et al. (2000, 2002b), using a randomly oriented spheroids model. We have used this approach when assessing the particle size distribution retrieval of dust aerosols. It is clear that care must be taken with the error associated with the particle size distribution and radiative parameters when using the Dubovik et al. (2000, 2002a) inversion method.

All available level 1.5 (as defined by AERONET protocols) radiance and AOD data were used to retrieve the volume size distribution function, dV/dlnr. Several representative days of the July–August desert dust episode are shown in Figs. 9a–d, where we can follow the evolution of aerosol particle size distributions in some detail. The particle size distributions always exhibit two modes: an accumulation mode, with particle radius below 0.6 μm, and a coarse mode, with particle radius between 0.6 and 15 μm. The coarse particle mode is always dominant during conditions where AOD is greater than 0.4. At the onset of the event, in the early morning of 29 July (Fig. 9a), when no dust is yet present, the maximum aerosol volume particle concentration (using the sphere model) is less than 0.02 $\mu m^3/\mu m^2$, with similar concentrations for both modes. For 30 July to 3 August the sphere model led to anomalous results for the accumulation mode, hence, we have used the spheroid model for the retrievals during this latter period.

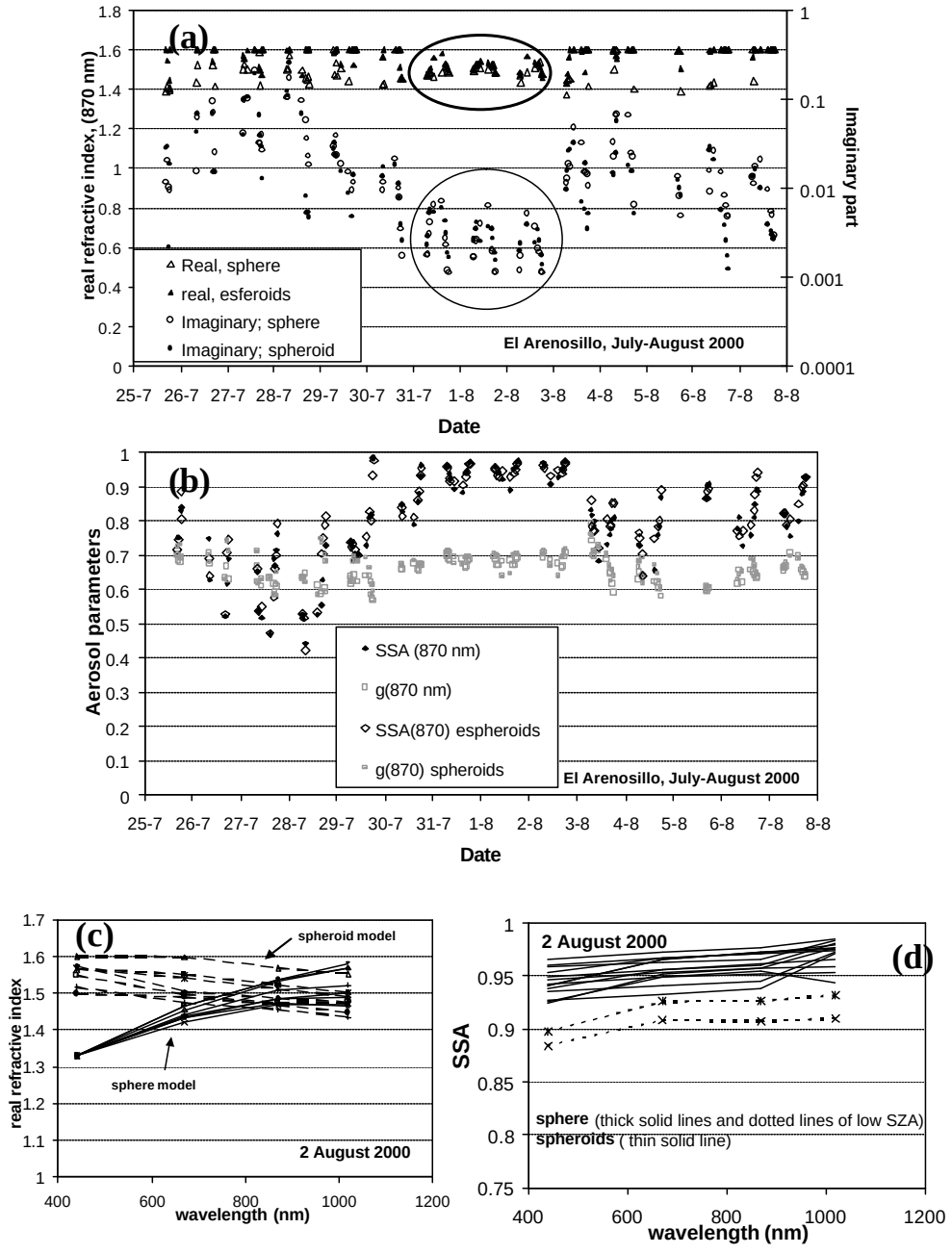

Fig. 10. Evolution of **(a)** the real and imaginary parts of the refractive index, **(b)** single scattering albedo and asymmetry parameter during the desert dust event of July–August at El Arenosillo, obtained by the AERONET inversion protocol. **(c)** Dependence on the wavelength of (c) the real part of the refractive index and d) single scattering albedo for sphere and spheroid models for day 2 August.

On 30 and 31 July, the coarse number concentration increases to 0.06 and 0.15 $\mu m^3/\mu m^2$, respectively (Fig. 9b), typical of values characteristic of desert aerosol. Figure 9c shows the size distribution on 1 August, with a maximum coarse mode concentration of 0.25 $\mu m^3/\mu m^2$, two orders of magnitude higher than on 29 July. The values for 3 August (Fig. 9d) and 4 August (not shown) decreased to those found for 29 July. For these two days, retrievals from both the sphere and spheroid models do not differ significantly. In addition to the two-orders of magnitude change in the volume size distribution during the dust event, the modal coarse radius decreased to 2–3 μm, compared to 5–6 μm for typical background conditions.

Results for desert aerosol type size distributions are discussed in Dubovik et al. (2002a; see references therein). Comparison of these distributions with our results is not

so straightforward, due to the variability in the intensity of dust events over our sites. Nevertheless, we conclude that the results are consistent with those reported by Dubovik et al. (2002a), because of the enhanced concentrations in the coarse mode. The results of Pinker et al. (2001) are also not directly comparable to our findings, as they were obtained close to the aerosol sources. Smirnov et al. (1998) reported data from the ACE2 experiment at Tenerife (Canary Islands) at two different altitudes (sea level and 2360 m at Izaña) during dust outbreaks. At Izaña, as an illustration, the AOD changes from 0.02 to 0.2, while the coarse mode size distribution concentration changed by two orders of magnitude and the modal radius changed from 0.8 to 2 μm. Thus, our volume concentration values of $\sim 0.2\,\mu m^3/\mu m^2$ for the coarse mode seem to be consistent with those reported by others (Smirnov et al., 1998; Dubovik et al., 2002a, b).

According to Dubovik et al. (2002a), retrieval of the refractive index is only reliable when AOD is greater than 0.4. This criterion was satisfied only for 31 July–2 August. Refractive index values are shown in Fig. 10 for both the sphere and spheroid retrieval models. Again, the sphere model values are generally valid for nondust conditions, while the spheroid model is better for dust. Similar features for both models are indicated in the real and imaginary parts of the refractive index, although with different values. The real part of the refractive index, n_R, ranges from 1.43–1.53 and the imaginary part, n_I, from 0.0013 to 0.006.

For reference, Dubovik et al. (2002a) give a range of values between 1.48–1.56 for n_R and 0.0006–0.001 for n_I (at 870 nm). Our values for n_R are within the same interval, but our values for n_I are greater. We comment on aerosol absorption later when discussing single scattering albedo (SSA) values.

With respect to the wavelength variation of n_R, we also found for the sphere model (see Fig. 10c for 2 August) the same dependence (increase with wavelength) described by Dubovik et al. (2000, 2002a, b). The values of 1.33 for n_R at 440 nm, however, seem unrealistic. In contrast to the sphere model, the spheroid model shows an inverse wavelength behaviour, with values decreasing with wavelength and a relatively large value at 440 nm. The two models agree for the two longer wavelengths (870 and 1020 nm, respectively).

The values for g and SSA at 870 nm are shown in Fig. 10b for the sphere and spheroid model retrievals, with g ranging from 0.64 to 0.71 and SSA from 0.88 to 0.97 during the three days. No significant differences are seen between the different model retrievals. Also, a slight diurnal dependence can be observed in the results (Fig. 10c) for SSA and to a lesser extent for g. In Fig. 10d for 2 August, we see an increase in SSA with wavelength, which seems to be a characteristic of desert aerosol (Dubovik et al., 2002a). Both sphere and spheroid model results agree except for low SZA (thick dotted line in Fig. 10d). This result indicates that SSA is well retrieved and not affected by the problems relative to the accumulation mode of the size distribution and real refractive index mentioned above.

Because aerosol light absorption is a key parameter in estimating climate aerosol forcing, comparison of our data with those of other studies is of great interest. As shown by Hansen et al. (1997) a change in SSA from 0.95 to 0.85 can change the radiative forcing from negative to positive, depending on the underlying surface. Although our values are quite variable, they are within the range obtained by Dubovik et al. (2002a), but indicating slightly high absorption. Indeed, Dubovik et al. (2002a) discuss the high SSA (less absorption) values retrieved at representative desert sites with respect to earlier established values in the literature (e.g. D'Almeida et al., 1991; Hess et al., 1998; WMO, 1983). As another, more recent example, Haywood et al. (2003), report on SSA values obtained from data collected during the SHADE campaign and using model calculations based on measured size distributions and n_I in the range 0.008–0.0015. For n_I=0.008, the retrievals for SSA are not as reliable as those for n_I=0.0015.

Satellite measurements also indicate less absorption than older literature for desert aerosols, as discussed by Kaufman et al. (2001) and Sinyuk et al. (2003). Because of this tendency observed in recent studies, it is clear that additional measurements are needed for the assessment of dust aerosol absorption properties. Our study certainly shows the variability of desert dust arriving over the southwestern part of the Iberian Peninsula as a result of the frequency and intensity of these events. We conclude that further continuous effort in monitoring and characterization is needed in this region. Such work is now being carried out by the AERONET-PHOTONS network.

5 Conclusions

Detection and evaluation of desert dust episodes in the southern part of the Iberian Peninsula during 2000 have been accomplished by means of three different types of measurements and analysis procedures, with remarkable agreement among them. Despite the known year-to-year variability, this evaluation gives some insight into the frequency of dust episodes and the number of days per year affected by desert dust over this region. It also provides information on the range of values of specific aerosol parameters such as AOD and α.

In general, the events at the end of winter are more intense, but less frequent and shorter in duration than those of summer which have a more extended and diluted dust plume, reinforced by low rainfall and re-circulations. While we have observed many one-day events with desert aerosol characteristics, it is often difficult to assign any of these days as belonging to a particular episode.

The detailed characterization of two dust case studies, using a combination of microphysical (particle size distribution and derived parameters) and optical properties, allowed the

determination of the range of these parameters in this coastal area of southwestern Spain.

Acknowledgements. We would like to thank the COST-ACTION 713 'UV-B Forecasting' and its organizer, A. Bais, for its financial support of the Short-term Scientific Mission: Relationship between the aerosol optical depth and derived properties in the UV and Visible ranges, related with aerosol types and air masses' led by R. Vergaz at Lisboa during November–December 2000, that allowed us to carry out this work. Also thanks are due to J. Gröbner from ECUV (JRC, Ispra) for providing comparative data of Brewer AOD and to CICYT (Spanish Commission for Research and Technology) for the financial support of Projects REN2000-0903-C08-04CLI and REN2002-00966. N. Laulainen was supported by the U.S. Department of Energy (DOE) under Contract DE-AC06-76RLO 1830. Pacific Northwest National Laboratory is operated by Battelle for the U.S. DOE.

Topical Editor F. D'Andrea thanks two referees for their help in evaluating this paper.

References

Arola, A. and Koskela, T.: On the sources of bias in aerosol optical depth retrieval in the UV range, J. Geophys. Res., 109, D08209, doi:10.1029/2003JD004375, 2004.

Artiñano, B., Querol, B., Salvador, P., Rodríguez, S., Alonso, D., and Alastuey, A.: Assessment of airborne particulate matter in Spain in response to the new EU-directive, Atmos. Environ., 35, Suplement No.1, S43–S53, 2001.

Avila, A., Queralt-Mitjans, I., and Alarcón, M.: Mineralogical composition of African dust delivered by red rains over northeastern Spain, J. Geophys. Res., 102, D18, 21 977–21 996, 1997.

Bergametti, G., Gomes, L., Coudé-Gaussen, G., Rognon, P., and Le Coustumer, M.: African dust observed over Canary Island: source region identification and transport pattern for some summer situations, J. Geophys. Res., 94, 14 855–14 864, 1989.

Cachorro, V. E., Toledano, C., de Frutos, A, Vilaplana, J. M., Romero, P. M., and Cuevas, E.: Retrieval of aerosol optical depth (AOD) by the Brewer instrument: Detection and correction of calibration problem by a new method, in: Eight Biennial Brewer Users Working Group Meeting, El Arenosillo, Huelva, Spain, http://www.woudc.org/publications_e.html, 2003.

Cakmur, R., Miller, R., and Tegen, I.: A comparison of seasonal and interannual variability of soil dust aerosol over the Atlantic ocean as inferred by TOMS and AVHRR AOT retrieval, J. Geophys. Res., 106, 18 287–18 304, 2001.

Cape, J., Methven, J., and Hudson, L.: The use of trajectory cluster analysis to interpret trace gas measurements at Mace Head, Ireland, Atmos. Environ., 34, 3651–3663, 2000.

Carvalho, F. and Henriques, D.: Use of Brewer ozone spectrophotometer for aerosol optical depth measurements on ultraviolet region., Adv. Space Res., 25(5), 997–1006, 2000.

Cheymol, A. and De Backer, H.: Retrieval of the aerosol optical depth in the UV-B at Uccle from Brewer ozone measurements over a long time period 1984–2002, J. Geophys. Res., 189(D24), 4800, doi:10.1029/2003JD007558, 2003.

D'Almeida, G., Koepke, P., and Shettle, E. P.: Atmospheric Aerosols: Global Climatology and Radiative Characteristics, A. Deepak Publishing, 1991.

Deepak A., and Gerber, H.: Report of the experts meeting on aerosols and their climatic effects. Technical Report WCP-55,World Meteorological Organization, Case Postal No. 5, CH-1211 Geneva, Switzerland, 107, 1983.

Derwent, R., Simmonds, P., Seuring, S., and Dimmer, C.: Observation and interpretation of the seasonal cycles in the surface concentrations of ozone and carbon monoxide at Mace Head, Ireland, from 1990 to 1994, Atmos. Environ., 32, 145–157, 1998.

Díaz, J., Expósito, F., Torres, C., Carreño, V., and Redondas, A.: Simulation of mineral dust effects on UV radiation levels, J. Geophys. Res., 105(D4), 4979–4991, 2000.

Díaz, J. P., Expósito, F. J., Torres, C. J., Herrera, F., Propero, J. M., and Romero, M. C.: Radiative properties of aerosols in Sarna dust outbreaks using ground-based and satellite data: Applications to radiative forcing., J. Geophys. Res., 106, D6, 18 433–18 416, 2001.

Draxler, R.: Boundary layer isentropic and kinematic trajectories during the August 1993 North Atlantic Regional Experiment Intensive, J. Geophys. Res., 101(D22), 29 255–29 268, 1996.

Draxler, R. and Hess, G. D.: Description of the HYSPLIT_4 modeling system, NOAA Technical Memorandum. Technical report, ERL ARL-224, December 1997.

Draxler, R. and Hess, G. D.: An overview of the HYSPLIT_4 modelling system for trajectories, dispersion and deposition, Aust. Met. Mag., 47, 295—308, 1998.

Dubovik, O. and King, M. D.: A flexible inversion algorithm for retrieval of aerosol optical properties from sun and sky radiance measurements, J. Geophys. Res., 105, 20 673–20 696, 2000.

Dubovik, O., Smirnov, A., Holben, B., King, M., Kaufman, Y., Eck, T., and Slutsker, I.: Accuracy assessments of aerosol optical properties retrieved from AERONET Sun and sky-radiance measurements, J. Geophys. Res., 105, 9791–9806, 2000.

Dubovik, O., Holben, B., Eck, T., Smirnov, A., Kaufman, Y., King, M., Tanré, D., and Slutsker, I.: Variability of absorption and optical properties of key aerosol types observed in worldwide locations. J. Atmos. Sci., 59, 590–608, 2002a.

Dubovik, O., Holben, B., Lapyonok, T., Sinyuk, A., Mishchenko, M., Yang, P., and Slutsker, I.: Non-spherical aerosol retrieval method employing light scattering by spheroids, Geophys, Res. Lett., 29(10), 1415, doi:10.1029/2001GLO15506, 2002b.

Eck, T., Holben, B., Reid, J., Dubovik, O., Smirnov, A., O'Neil, N., Slutsker, I., and Kinne, S.: Wavelength dependence of the optical depth of biomass burning, urban, and desert dust aerosols, J. Geophys. Res., 106, 31 333–31 349, 1999.

Ginoux, P., Chin, M., Tegen, I., Prospero, J., Holben, B., Dubovik, O., and Lin, S.: Sources and distribution of dust aerosols simulated with the GOCART model, J. Geophys. Res., 106(D17), 20 255–20 273, 2001.

Gröbner, J., Vergaz, R., Cachorro, V. Henriques, D., Lamb, K., Redondas, A., Vilaplana, J. M., and Rembges, D.: Intercomparison of aerosol optical depth measurements in the UVB using Brewer spectrophotometers and a Li-Cor spectrophotometer, Geophys. Res. Lett., 28(9), 1691–1694, 2001.

Groebner, J. and Meleti, C. : Aerosol optical depth in the UVB and visible from Brewer spectrophotometer direct irradiance measurements: 1991 to 2002, J. Geophys. Res., 109(D9), D09202, doi:10.1029/2003JD004409, 2004.

Guerzoni, S., Molinaroli, E., and Chester, R.: Sahara dust inputs to the western Mediterranean see: deposition pattern, geochemistry

and sedimentalogical implications, Atmos. Environ., 44, 631–654, 1997.

Hansen, J., Sato, M., and Ruedi, R.: Radiative forcing and climate response, J. Geophys. Res., 102, 6831–6864, 1997.

Haywood, J. and Boucher, O.: Estimates of direct and indirect radiative forcing due to tropospheric aerosols: A review, Rev. Geophys., 38, 513–543, 2000.

Haywood, J., Francis, P., Glew, M., and Taylor, J.: Optical properties and direct radiative effect of Saharan dust: A case study of two Saharan outbreak using aircraf data., J. Geophys. Res., 106, 18 417–18 430, 2001.

Haywood, J., Francis, P., Osborne, S., Glew, M., Loeb, N., Highwood, E., Tanré, D., Myhre, G., Formenti, P., and Hirst, E.: Radiative properties and direct radiative effect of Saharan dust measured by the C-130 aircraft during SHADE: 1. Solar Spectrum, J. Geophys. Res., 108(D18), 8577–8593, doi:10.1029/2002JD002687, 2003.

Herman, J. R., Barthia, P. K., Torres, O., Hsu, C., Setfor, C., and Celarier, E.: Global distribution of UV-absorbing aerosols from Nimbus 7/TOMS data, J. Geophys. Res., 102, 16 889–16 909, 1997.

Hess, M., Koepke, P., and Schult, I.: Optical Properties of Aerosols and Clouds: The Software Package OPAC, Bull. Am. Met. Soc., 79, 831–844, 1998.

Holben, B., Eck, T., Slutsker, I., Tanré, D., Buis, J., Setzer, A., Vermote, E., Reagan, J., and Kaufman, Y.: AERONET – a federated instrument network and data archive for aerosol characterization, Remote Sens. Environ., 66, 1–16, 1998.

Holben, B., Tanré, D., Smirnov, A., Eck, T., Slutsker, I., Abuhassan, N., Newcomb, W., Schafer, J., Chatenet, B., Lavenue, F., Kaufman, Y., Vande Castle, J., Setzer, A., Markham, B., Clark, D., Frouin, R., Halthore, R., Karnieli, A., O'Neill, N., Pietras, C., Pinker, R., Voss, K., and Zibordi, G.: An emerging ground-based aerosol climatology: Aerosol Optical Depth from AERONET, J. Geophys. Res., 106, 12 067–12 097, 2001.

Hsu, N., Herman, J., Torres, O., Holben, B., Tanré, D., Eck, T., Smirnov, A., Chatenet, B., and Lavenu, F.: Comparison of the TOMS aerosol index with sun photometer aerosol optical thickness: results and applications, J. Geophys. Res., 104, 6269–6279, 1999.

Husar, R. B., Tratt, D. M., Schnichtel, B. A., et al.: Asian dust events of April 1998, J. Geophys. Res., 106(D16), 18 317–18 330, 2001.

Jaroslawsky, J., Krzyscin, J., Puchalsky, S., and Sobolewski, P.: On the optical thickness in the UV range: Analysis of the ground-based data taken at Belsk, Poland, J. Geophys. Res., 108(D23), 4722, doi:10.1029/2003JD003571, 2003.

Karyampudy, V., Palm, S. Reagen, J., Hui Fang, Grant, W., Hoff, R., Moulin, C., Pierce, H., Torres, O., Browell, E., and Melfi, E.: Validation of the Saharan dust plume conceptual model using Lidar, Meteosat and ECMWF data, Bull. Am. Met. Soc., 80, 1045–1075, 1999.

Kaufman, Y., Tanré, D., Dubovik, O., Karnieli, A., and Remer, L. A.: Absorption of sunlight by dust as inferred from satellite and ground-based remote sensing, Geophys. Res. Lett., 28, 1479–1482, 2001.

Kazadzis, S., Bais, A., Kouremeti, N., Garasopoulos, E., Garane, K., Blumthaler, M., Schallhart,B., and Cede, A: Direct spectral measurements with a brewer spectroradiometer: absolute calibration and aerosol optical depth retrieval, Appl. Opt., 44, 1681–1690, 2005.

Kerr, J.: New methodology for deriving total ozone and other atmospheric variables from Brewers spectrophotometer direct sun spectra, J. Geophys. Res., 107(D23), 4731, doi:10.1029/2002JD001227, 2002.

Kerr, J., McRoy, C., and Olafson, R.: Measurements of ozone with Brewer ozone spectrophotometer, in: Proc. Quadrennial Int. Ozone Symp., 74–79, 1981.

Kinne, S., Holben, B., Eck, T., Smirnov, A., Dubovik, O., Slutsker, I., Tanre, D., Zibozdi, G., Lohmann, U., Ghan, S., Easter, R., Chin, M., Ginoux, P., Takemura, T., Tegen, I., Koch, D., Kahn, R., Vermote, E., Stowe, L., Torres, O., Mishchenko, M., Geogdzhayev, I., and Hiragushi, A.: How well do aerosol retrievals from satellites and representation in global circulation models match ground-based AERONET aerosol statistics? in: Remote Sensing and Climate Modeling: Synergies and Limitations, edited by: Beniston, M. and Verstraete, M., vol. 7 of Advances in Global Change Research Kluwer Academic, Dordrecht, Netherlands, 103–158, 2001.

Kirchhoff, V., Silva, A., Costa, C., Paes Lem, N., Pavao, H., and Zaratti, F.: UVB optical thickness observations of the atmosphere, J. Geophys. Res., 106, 2963–2973, 2001.

Longtin, D., Shettle, E., Hummel, J., and Pryce, J.: A desert aerosol model for radiative transfer studies, Aerosols and Climate, A. Deepak, Hampton, Va, 261–269, 1988.

Marenco, F., di Sarra, A., and de Luisi, J.: Methodology for determining aerosol optical depth from Brewer 300–320 nm measurements, *Appl. Opt.*, 41, 1805–1814, 2002.

McPeters, R., Bhartia, P., Krueger, A., and Herman, J.: Earth Probe Total Ozone Mapping Spectrometer (TOMS) Data Products Users Guide, Technical report, NASA Technical Publication, 1998.

Miller, R. and Tegen, I.: Climate response to soil dust aerosol, J. Climate, 11, 3247–3267, 1998.

Moulin, C., Guillard, F., Dulac, F., and Lambert, C.: Long-term daily monitoring of Saharan dust load over ocean using Meteosat ISCCP-B2 data: Methodology and preliminary results for 1983–1994 in the Mediterranean, J. Geophys. Res., 102, 16 947–16 958, 1997a.

Moulin, C., Lambert, C., Dayan, U., and Dulac, F.: Control of atmospheric export of dust from North Africa by the North Atlantic oscillation, Nature, 387, 691–694, 1997b.

Pinker, R., Pandithurai, G., Holben, H., Dubovik, O., and Aro, T.: A dust outbreak in sub-Sahel West Africa, J. Geophys. Res., 106, 22 923–22 930, 2001.

Prospero, J.: The Impact of Desert Dust Across the Mediterranean, Saharan dust transport over the North Atlantic Ocean and Mediterranean: An overview, Kluwer Acad., Norwell, Mass, 131–151, 1996.

Prospero, J.: Long range transport of mineral dust in the global atmosphere: impact of African dust on the environment of Southeastern United States, Proc. Nat. Acad. Sci. USA, 96, 3396–3403, 1999.

Querol, X., Rodriguez, S., Cuevas, E., Viana, N. M., and Alastuey, A.: African air mass intrusions over the Iberian Peninsula and the Canary Islands: Transport pattern and seasonal trends, in 3a Asamblea Hispano Lusa de Geofísica y Geodesia, Proceeding Tomo II, 84–88 (S13), 12 (ISBN: 84-9705-299-4), 2002a.

Querol, X., Alastuey, A., Sánchez de la Campa, A., de la Rosa, J., Plana, F., and Ruiz, C.: Source apportionment analysis of atmospheric particulates in an industrialised urban site in Southwestern Spain, Atmos. Environ., 36, 3113–3125, 2002b.

Rodríguez, S., Querol, X., Alastuey, A., Kallos, G., and Kakaliagou, O.: Saharan dust contributions to PM10 and TSP levels in Southern and Eastern Spain, Atmos. Environ., 35, 2433–2447, 2001.

Sánchez de la Campa, A.: Impacto de material particulado atmosférico norteafricano en Andalucia. Research report of third cycle, Departamento de Geología, University of Huelva, 2002.

Shine, K. and Forster, F.: The effects of human activity on radiative forcing of climate change: A review of recent developments, Global Planet. Change, 20, 205–225, 1999.

Sinyuk, A., Torres, O., and Dubovik, O.: Combined use of satellite and surface observations to infer the imaginary part of refractive index of Sahara dust, Geophys. Res. Lett., 30(2) 1081, doi:10.1029/2002GLO16189, 2003.

Smirnov, A., Holben, B., Slutsker, I., Welton, E., and Formenti, P.: Optical properties of Saharan dust during ACE-2, J. Geophys. Res., 103, 28 079–28 092, 1998.

Smirnov, A., Holben, B., Eck, T., Dubovik, O., and Slutsker, I.: Cloud screening and quality control algorithms for the AERONET database, Remote Sens. Environ., 73, 337–349, 2000.

Stohl, A.: Computation, accuracy and applications of trajectories: a review and bibliography, Atmos. Environ., 32(6), 947–966, 1998.

Stowe, L., Ignatov, A., and Singh, R.: Development, validation and potential enhancements to the second generation operational aerosol product at the National Environmental satellite, Data, and Information Services of the National Oceanic and Atmospheric administration, J. Geophys. Res., 102, 16 923–16 934, 1997.

Stunder, B.: An assessment of the quality of forecast trajectories, J. Appl. Meteorol., 35, 1319–1331, 1996.

Tanré, D., Kaufman, Y., Herman, M., and Mattoo, S.: Remote sensing of aerosol properties over ocean using the MODIS/EOS spectral radiances, J. Geophys. Res., 102(D14), 16 971–16 988, 1997.

Tegen, I. and Lacis, A.: Modeling of particle size distribution and its influence on the radiative properties of mineral dust aerosol, J. Geophys. Res., 101, 19 237–19 244, 1996.

Tegen, I., Lacis, A., and Fung, I.: The influence on climate forcing of mineral aerosols from disturbed soils, Nature, 380, 419–422, 1996.

Torres, O. and Barthia, P.: Impact of tropospheric aerosol absorption on ozone retrieval from backscattered ultraviolet measurements, J. Geophys. Res., 104, 21 569–21 577, 1999.

Vergaz, R.: Propiedades ópticas de los aerosoles atmosféricos, Caracterización del área del Golfo de Cádiz, PhD Thesis, Universidad de Valladolid, Spain, 2001.

Vergaz, R., Cachorro, V., de Frutos, A., Henriques, D., Vilaplana, J., and de la Morena, B.: Columnar characteristics of aerosols in the maritime area of the Cádiz Gulf (Spain), Int. J. Climatol., 25, 1793–1804, doi:101002/joc.1208, 2005.

Vilaplana, J., Sorribas, M., Luccini, E., Vergaz, R., Cachorro, V., Piacentini, R., de la Morena, B., Gonzalez-Frías, C., and de Frutos, A.: Calibration of a Yankee UVB-1 Biometer Based on Spectral Measurements with a Double-Monocromator Brewer Spectrophotometer, in: 3a Asamblea Hispano-Portuguesa de Geodesia y Geofísica, volume II, 1204–08 (S13)(ISBN: 84-9705-299-4), 2002.

Vilaplana, J.: Medida y análisis del ozono y de la radiación solar ultravioleta en El Arenosillo-INTA, (Huelva), PhD Thesis, Department of Optics, University of Valladolid, Spain, 2004.

Wang, M., Bailey, S., MacClain, C., Pietras, C., and Riley, T.: Remote sensing of the aerosol optical thickness from SeaWIFS in comparison with the in situ measurements, In ALPS99: The Contribution of POLDER and New Generation Spaceborne Sensors to Global Change Studies, Meribel, France, WK1-O-08, 1999.

WMO: Radiation Commission of IAMAP meeting of experts on aerosol and their climatic effects, Technical Report Rep, WCP55, World Meteorological Organization, 1983.

Yankee: Yankee Users Guide of Ultraviolet Piranometer model UVB-1/UVA-1. Yankee Environmental System Inc., 1996.